The Σ^- states of the molecular hydrogen

Jacek Komasa*

Received 29th February 2008, Accepted 2nd April 2008
First published as an Advance Article on the web 8th May 2008
DOI: 10.1039/b803548b

A class of doubly excited electronic states of the hydrogen molecule is reported. The states are of Σ^- symmetry and are located *ca.* 200 000 cm^{-1} above the ground state and about 75 000 cm^{-1} above the ionization threshold. The electronic wave functions employed to described these states have been expanded in the basis of exponentially correlated Gaussian (ECG) functions with the nonlinear parameters variationally optimized. The lowest $^3\Sigma_g^-$ and $^1\Sigma_u^-$ states dissociate into hydrogen atoms in the $n = 2$ state, whereas the lowest $^3\Sigma_u^-$ and $^1\Sigma_g^-$ states have H($n = 2$) and H($n = 3$) as the dissociation products. All the four states are attractive and accommodate vibrational levels. The location of the vibrational energy levels has been determined by solving the radial Schrödinger equation within the Born–Oppenheimer approximation.

I. Introduction

In diatomic molecules any plane containing the nuclei is a plane of symmetry σ_v. An electronic wave function of a Σ state under reflection in such a plane either remains unchanged ($\sigma_v\psi = \psi$) or changes the sign ($\sigma_v\psi = -\psi$). The state described by the wave function having the latter property is labelled Σ^-. Well-known examples of homonuclear diatomic molecules having the Σ^- symmetry of their ground states are B_2 and O_2. To the author's knowledge there are no published numerical data, neither theoretical nor experimental, concerning the Σ^- states of H_2.

A simple two-electron wave function of Σ^- symmetry can be composed of atomic real p orbitals perpendicular to the molecular axis. Assuming that the molecule lies along the X axis, such a wave function could be described as $p_y(1)p_z(2) - p_z(1)p_y(2)$. Of course, this is not the only combination of atomic orbitals suitable to construct a Σ^- wave function—other examples are $p_y(1)d_{xz}(2) - p_z(1)d_{xy}(2)$ or $d_{xy}(1)d_{xz}(2) - d_{xz}(1)d_{xy}(2)$. Many other instances involving d and f orbitals can be found in ref. 1.

The Σ^- states of the hydrogen molecule arise from double excitation. In H_2 the double excited states, of any symmetry, are of great interest for their ability to autoionize or to dissociate into neutral excited hydrogen atoms. A variety of possible decay channels enables their analysis by a multitude of experimental techniques complementary to each other: radiative association, electron impact excitation, multiphoton absorption, electron scattering and others.

Doubly excited states are usually much more difficult to describe quantum-mechanically than the ground or low lying excited states. The reason is the exceptionally important role the electron correlation plays in the binding of the system. The two excited electrons move slower than in a ground state and their response to the mutual Coulomb repulsion is greater, which increases a need for proper description of the electron correlation effect.

Faculty of Chemistry, A. Mickiewicz University, Grunwaldzka 6, 60-780 Poznań, Poland. E-mail: komasa@man.poznan.pl

The purpose of this paper is to report on the theoretically predicted shape and location on the energy scale of the lowest Σ^- electronic states and their vibrational levels using highly accurate explicitly correlated wave functions.

II. Methodology

A The Born–Oppenheimer approximation

The results reported in this paper have been obtained within the frames of the Born–Oppenheimer approximation. The total wave function Ψ was assumed as a product of the electronic and nuclear functions

$$\Psi(\boldsymbol{r},\boldsymbol{R}) = \Phi(\boldsymbol{r};R)\chi(R)Y(\theta,\phi)/R. \tag{2.1}$$

The electronic wave function Φ depends parametrically on the internuclear distance R and, for each R separately, it is a solution to the electronic Schrödinger equation

$$\hat{H}\Phi(\boldsymbol{r};R) = E(R)\Phi(\boldsymbol{r};R) \tag{2.2}$$

with the clamped nuclei Hamiltonian (in atomic units)

$$\hat{H} = -\frac{1}{2}\sum_{i=1}^{2}\nabla_i^2 + \frac{1}{|\boldsymbol{r}_i - \boldsymbol{r}_j|} - \sum_{I=1}^{2}\sum_{i=1}^{2}\frac{1}{|\boldsymbol{r}_i - \boldsymbol{R}_I|} + \frac{1}{|\boldsymbol{R}_1 - \boldsymbol{R}_2|}. \tag{2.3}$$

The $r_i = (x_i,y_i,z_i)$ and $\boldsymbol{R}_I$ are the ith electron and the Ith nucleus position vectors, respectively. The functions χ_v are eigensolutions to the radial Schrödinger equation

$$\left[-\frac{1}{M_p}\frac{\mathrm{d}^2}{\mathrm{d}R^2} + E(R)\right]\chi_v(R) = E_v\chi_v(R), \tag{2.4}$$

where the eigenvalues E_v represent the rotationless vibrational energy levels with the proton mass M_p.

B The electronic wave function

The electronic Schrödinger eqn (2.2) has been solved variationally using the Ritz method. The trial wave function Φ has been expanded in the form of an antisymmetrized, K-term,

Table 1 Convergence of the energy (in E_H) of the Σ^- states of H_2 at their equilibrium distances

K	$E(^1\Sigma_g^-)$	$E(^1\Sigma_u^-)$	$E(^3\Sigma_g^-)$	$E(^3\Sigma_u^-)$
75	−0.192 373 856	−0.250 079 899	−0.267 881 560	−0.204 310 132
150	−0.192 374 268	−0.250 079 953	−0.267 882 116	−0.204 311 343
300	−0.192 374 300	−0.250 079 959	−0.267 882 165	−0.204 311 521
600	−0.192 374 306	−0.250 079 960	−0.267 882 173	−0.204 311 528
∞	−0.192 374 308(1)	−0.250 079 961(1)	−0.267 882 175(1)	−0.204 311 530(2)

linear combination of two-electron basis functions

$$\Phi(\boldsymbol{r}_1,\boldsymbol{r}_2) = (1 \pm \hat{P}_{12})(1 \pm \hat{\imath}) \sum_{k=1}^{K} c_k \phi_k(\boldsymbol{r}_1,\boldsymbol{r}_2). \qquad (2.5)$$

The $\hat{P}_{12}$ is the electron exchange operator, and the *plus* or *minus* sign in front of it represents implicitly a singlet or triplet state, respectively. The $1 \pm \hat{\imath}$ projector ensures that the wave function transforms properly under the inversion operation. The *plus* sign within the projector generates the *gerade* states and the *minus* sign—the *ungerade* states. Different combinations of the two projectors lead to the four states of $^1\Sigma_g^-$, $^1\Sigma_u^-$, $^3\Sigma_g^-$, and $^3\Sigma_u^-$ symmetry.

The basis functions ϕ_k were taken in the form of exponentially correlated Gaussian (ECG) functions,[2,3] which in the particular two-electron case are known also as Gaussian-type geminals (GTG).[4–9] In order to constrain the solutions of the Schrödinger equation to the Σ^- states, the spatial functions have been imposed this particular symmetry. The explicit form of the basis function, assuming that the nuclei are placed along the X axis, reads

$$\phi_k(\boldsymbol{r}_1,\boldsymbol{r}_2) = (y_1 z_2 - z_1 y_2) \times \exp\left[-\sum_{i,j=1}^{2} \boldsymbol{A}_{ij,k}(\boldsymbol{r}_i - \boldsymbol{s}_{i,k})(\boldsymbol{r}_j - \boldsymbol{s}_{j,k})\right], \qquad (2.6)$$

where the matrices $\boldsymbol{A}_k$ and vectors $\boldsymbol{s}_k$ contain nonlinear parameters, 5 per basis function, to be determined variationally.

The optimum linear parameters c_k were found by means of the inverse iteration algorithm of solving the standard general symmetric eigenvalue problem. The K-term wave function Φ depends also on the set of $5K$ nonlinear parameters, which for K of the order of hundreds makes the function very flexible but, simultaneously, the energy minimum has to be searched for in a large space with dimensions of the order of a couple of thousands. The nonlinear parameters were optimized for each R independently with respect to the lowest root of each

Table 2 The singlet Σ^- states of H_2 predicted using the 600-term ECG wave function

$^1\Sigma_g^-$			$^1\Sigma_u^-$		
R/bohr	E/E_H	dE/dR	R/bohr	E/E_H	dE/dR
0.000	He $2p3p\,^1$P		0.000	He $2p3d\,^1$D	
0.010	99.419 757 493	−9999.999 947 6	0.010	99.436 194 360	−10001.436 773 9
0.100	9.420 11 1819	−99.992 962 8	0.100	9.436 538 342	−99.996 466 1
0.500	1.428 011 189	−3.969 314 1	0.500	1.443 321 353	−3.973 632 0
1.000	0.447 708 923	−0.954 281 2	1.000	0.460 083 769	−0.961 498 9
1.500	0.138 619 441	−0.394 416 6	1.500	0.146 864 968	−0.403 604 1
2.000	−0.003 096 080	−0.200 755 0	2.000	0.000 181 626	−0.211 360 1
2.500	−0.079 141 586	−0.113 625 4	2.500	−0.081 423 895	−0.125 181 5
3.000	−0.123 499 338	−0.068 298 5	3.000	−0.131 696 521	−0.080 319 6
3.500	−0.150 625 150	−0.042 456 0	3.500	−0.164 849 062	−0.054 467 5
4.000	−0.167 624 403	−0.026 774 7	4.000	−0.187 767 089	−0.038 382 0
4.500	−0.178 345 118	−0.016 830 3	4.500	−0.204 130 614	−0.027 759 0
5.000	−0.185 022 106	−0.010 322 4	5.000	−0.216 067 938	−0.020 418 1
5.500	−0.189 024 010	−0.005 970 4	6.000	−0.231 474 810	−0.011 337 5
6.000	−0.191 224 858	−0.003 022 1	7.000	−0.240 079 411	−0.006 346 3
6.500	−0.192 202 319	−0.001 016 6	8.000	−0.244 874 638	−0.003 506 6
6.860	−0.192 374 306	0.000 012 2	9.000	−0.247 493 599	−0.001 883 2
7.000	−0.192 349 321	0.000 338 5	10.000	−0.248 875 199	−0.000 969 1
7.500	−0.191 940 111	0.001 233 9	11.000	−0.249 568 701	−0.000 469 6
8.000	−0.191 170 510	0.001 797 4	12.000	−0.249 893 088	−0.000 208 3
9.000	−0.189 085 132	0.002 250 6	13.000	−0.250 028 830	−0.000 079 0
10.000	−0.186 857 353	0.002 133 8	14.000	−0.250 074 109	−0.000 019 7
11.000	−0.184 924 656	0.001 693 2	14.940	−0.250 079 960	0.000 003 7
12.000	−0.183 523 275	0.001 093 8	15.000	−0.250 079 711	0.000 004 6
13.000	−0.182 744 907	0.000 478 6	20.000	−0.250 026 297	0.000 007 1
14.000	−0.182 473 848	0.000 127 1	25.000	−0.250 007 318	0.000 001 7
15.000	−0.182 393 273	0.000 061 8	100.000	−0.250 000 002	0.000 000 0
16.000	−0.182 323 326	0.0000829	∞	−0.250 000 000	H($2p$) + H($2p$)
18.000	−0.182 101 357	0.000 132 9			
20.000	−0.181 820 642	0.000 141 6			
25.000	−0.181 237 613	0.000 085 9			
100.000	−0.180 564 618	0.000 000 3			
∞	−0.180 555 556	H($2p$) + H($3p$)			

symmetry. The parameters of every single basis function were selected from a large set of randomly generated numbers on the basis of yielding the lowest energy. The selected 5 parameters were further optimized using Powell's conjugate directions method[10] while all the remaining parameters were kept frozen. The same procedure was applied to every new basis function until the expansion of the assumed size was built. The wave function in its final size was further optimized in a similar fashion—the Powell procedure was applied subsequently to all expansion terms, forming a single cycle of the optimization. The energy gain from a cycle was used as a parameter controlling the convergence—the cycles were repeated as long as the energy gain decreased to a fraction of nanohartree (nE_H). Detailed description of the ECG method including the optimization strategy employed here may be found *e.g.* in ref. 11–14.

III. Results and discussion

In order to assess the accuracy of the energy curves reported, we performed the convergence test at the equilibrium distances of all four states. Table 1 shows how the energy approaches the Born–Oppenheimer energy limit when the basis set size K is successively doubled. On the basis of this data we extrapolated the energy to the limit of an infinite expansion and estimated the missing part of the energy to be of the order of a few nanohartree. Analogous tests made at short and long internuclear distances revealed the same order of magnitude of the error.

The final electronic calculations have been performed using 600-term ECG wave functions at a wide range of internuclear distances R, including very short (R = 0.01 bohr) and very long distances (R = 100.0 bohr). The knowledge of the limiting values enables us to correlate precisely the energy curves with the united atom (UA) and separate atoms (SA) limits. The Born–Oppenheimer energies of the four Σ^- states are presented in Tables 2 and 3. In addition, at every distance R the derivative dE/dR, helpful in an interpolation of the potential energy function, is given. The derivative has been computed using the expectation value of the electronic kinetic energy T and the formula

$$\left.\frac{dE}{dR}\right|_R = -\frac{E+T}{R} \qquad (3.7)$$

resulting from the virial theorem and applicable only to very accurate wave functions. Fig. 1 shows a general view of the predicted electronic Σ^- states in relation to the location of the ground states of H_2 and H_2^+. Detailed shapes and mutual positions of the four studied Σ^- states are shown in Fig. 2.

Table 3 The triplet Σ^- states of H_2 predicted using the 600-term ECG wave function

$^3\Sigma_g^-$			$^3\Sigma_u^-$		
R/bohr	E/E_H	dE/dR	R/bohr	E/E_H	dE/dR
0.000	He $2p^2\,^3P_e$		0.000	He $2p3d\,^3D$	
0.010	99.289 504 203	−9999.999 128 7	0.010	99.440 675 000	−9999.999 347 4
0.100	9.289 933 731	−99.991 356 9	0.100	9.440 996 567	−99.993 531 2
0.500	1.299 556 310	−3.962 491 2	0.500	1.448 161 050	−3.972 199 7
1.000	0.323 785 137	−0.943 469 7	1.000	0.465 955 582	−0.958 822 4
1.500	0.020 567 890	−0.382 056 0	1.500	0.154 369 392	−0.399 759 9
2.000	−0.114 894 848	−0.188 271 8	2.000	0.009 882 234	−0.206 444 0
2.500	−0.184 827 582	−0.101 736 2	2.500	−0.069 039 459	−0.119 409 6
3.000	−0.223 460 971	−0.057 322 0	3.000	−0.116 279 744	−0.074 023 3
3.500	−0.245 352 989	−0.032 505 5	3.500	−0.146 229 667	−0.048 011 8
4.000	−0.257 637 480	−0.017 863 4	4.000	−0.165 946 367	−0.032 075 9
4.500	−0.264 156 173	−0.008 926 2	4.500	−0.179 239 374	−0.021 808 1
5.000	−0.267 123 066	−0.003 377 5	5.000	−0.188 312 963	−0.014 923 3
5.490	−0.267 882 173	0.000 012 0	5.500	−0.194 512 745	−0.010 155 7
6.000	−0.267 282 131	0.002 151 1	6.000	−0.198 696 906	−0.006 766 7
7.000	−0.264 050 570	0.003 900 9	6.500	−0.201 433 420	−0.004 307 0
8.000	−0.260 055 451	0.003 89 48	7.000	−0.203 110 991	−0.002 493 1
9.000	−0.256 518 672	0.003 104 9	7.500	−0.204 003 050	−0.001 140 2
10.000	−0.253 907 616	0.002 121 5	8.000	−0.204 307 188	−0.000 124 3
11.000	−0.252 221 228	0.001 292 9	8.060	−0.204 311 528	−0.000 020 6
12.000	−0.251 231 190	0.000 731 2	9.000	−0.203 698 393	0.001 214 7
15.000	−0.250 225 630	0.000 116 5	10.000	−0.202 074 980	0.001 955 8
20.000	−0.250 029 023	0.000 009 3	11.000	−0.199 907 653	0.002 331 2
25.000	−0.250 007 350	0.000 001 8	12.000	−0.197 489 529	0.002 474 1
100.000	−0.250 000 002	0.000 000 0	13.000	−0.195 010 198	0.002 463 6
∞	−0.250 000 000	H(2p) + H(2p)	14.000	−0.192 597 224	0.002 347 5
			15.000	−0.190 340 658	0.002 154 7
			16.000	−0.188 307 125	0.001 904 1
			17.000	−0.186 546 352	0.001 612 2
			18.000	−0.185 089 542	0.001 300 3
			19.000	−0.183 942 910	0.000 997 0
			20.000	−0.183 082 928	0.000 731 2
			22.000	−0.182 023 201	0.000 366 1
			25.000	−0.181 332 982	0.000 137 9
			100.000	−0.180 564 619	0.000 000 3
			∞	−0.180555556	H(2p) + H(3d)

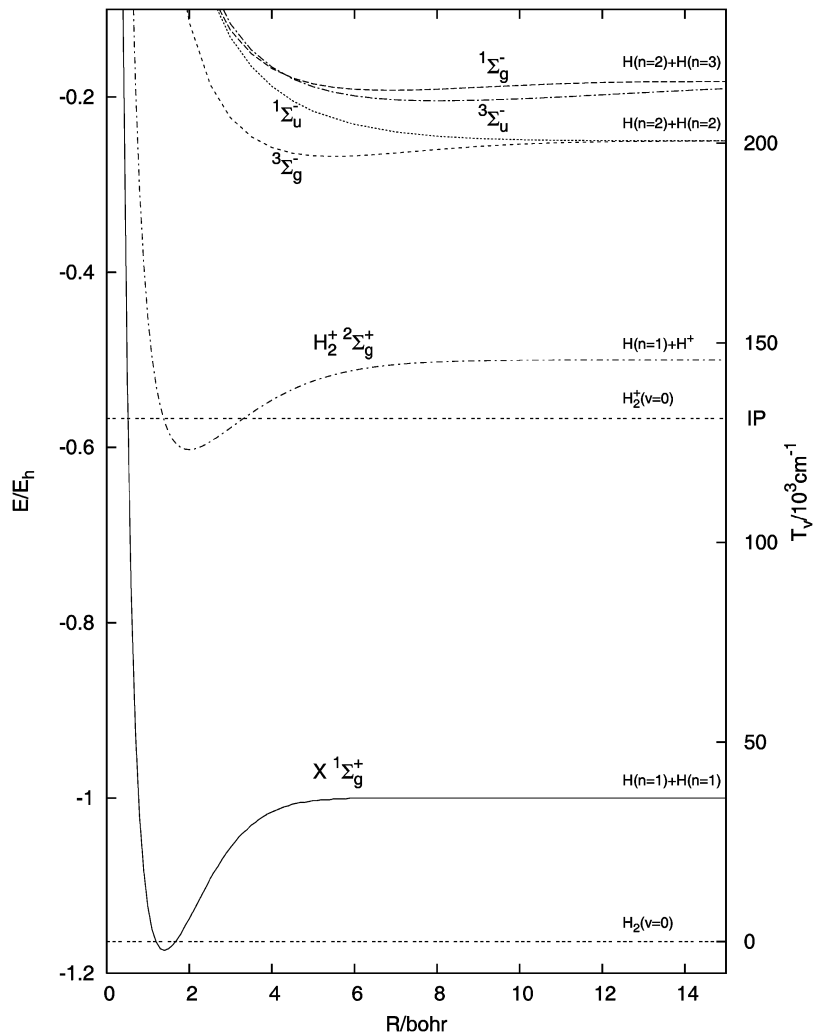

Fig. 1 General view of the Born–Oppenheimer energy curves of the Σ^-states of H_2 in relation to the ground state of H_2 and H_2^+.

Another quantity of our interest is the electronic energy $E_{el} = E - 1/R$, which can be easily inferred from the data listed in Tables 2 and 3. Contrary to the total energy E, the electronic energy is free of the $1/R$ term and contains no pole at $R = 0$. The finite value at $R \to 0$ makes E_{el} a quantity helpful in determining the UA limit corresponding to a given molecular state. Fig. 3 presents the dependence of E_{el} on R in the shortest range of internuclear distances. For $R \to 0$ the $E_{el}(R)$ goes precisely to the well known (see *e.g.* ref. 15–17) atomic energies of various doubly excited states of helium which, in turn, allows an unequivocal assignment of the UA configuration to particular states of H_2.

At the other end of $R \to \infty$, the Σ^- states of H_2 decay either into two hydrogen atoms in the $n = 2$ state or into one atom in the $n = 2$ and the other in $n = 3$ state. The same dissociation limits have the so-called Q_2 states of different symmetries placed between the second (H_2^+ $^2\Sigma_u^+$) and the third (H_2^+ $^2\Pi_u$) ionization limits.[18] The energy of the dissociation products can be found in Tables 2 and 3 or read from Fig. 2.

The lowest of the four states is the triplet *gerade* state. At the UA limit it correlates with $2p^2\ ^3P^e$ state of the helium atom ($E = -0.71050\ E_H$[15,17])—the lowest P state of even parity, whereas at the SA limit—with two hydrogen atoms both in $2p$ excited state. At the equilibrium distance $R_e = 5.49$ bohr the interaction potential is almost 4000 cm^{-1} deep. This state has 13 vibrational levels, the $v = 0$ level lying *ca.* 2×10^5 cm^{-1} above the ground vibronic level.

Next in the energy order is the singlet *ungerade* state. It has the same dissociation products as the $^3\Sigma_g^-$ state but its UA configuration corresponds to He($2p3d\,^1$D) of the energy $E = -0.56380\ E_H$.[16] It is the least attractive of all four states reported. The interaction energy curve is very shallow—its minimum, located far away at 14.94 bohr, is merely 18 cm^{-1} deep. Nevertheless, it accommodates one vibrational level with five rotational levels, the highest being quasi-bound.

The potential energy curve of the third state is the deepest (over 5200 cm^{-1} at $R = 8.06$ bohr) of all the four states and has about 40 vibrational levels. Because the potential well is very wide, the density of the vibrational levels right below the dissociation limit is relatively high and their number is difficult to determine precisely. This state dissociates into two hydrogen atoms, one in $2p$ and the other in $3d$ state. At $R \to 0$ it correlates with the $2p3d\,^3$D state of the helium atom which has the energy $E = -0.55933\ E_H$.[16]

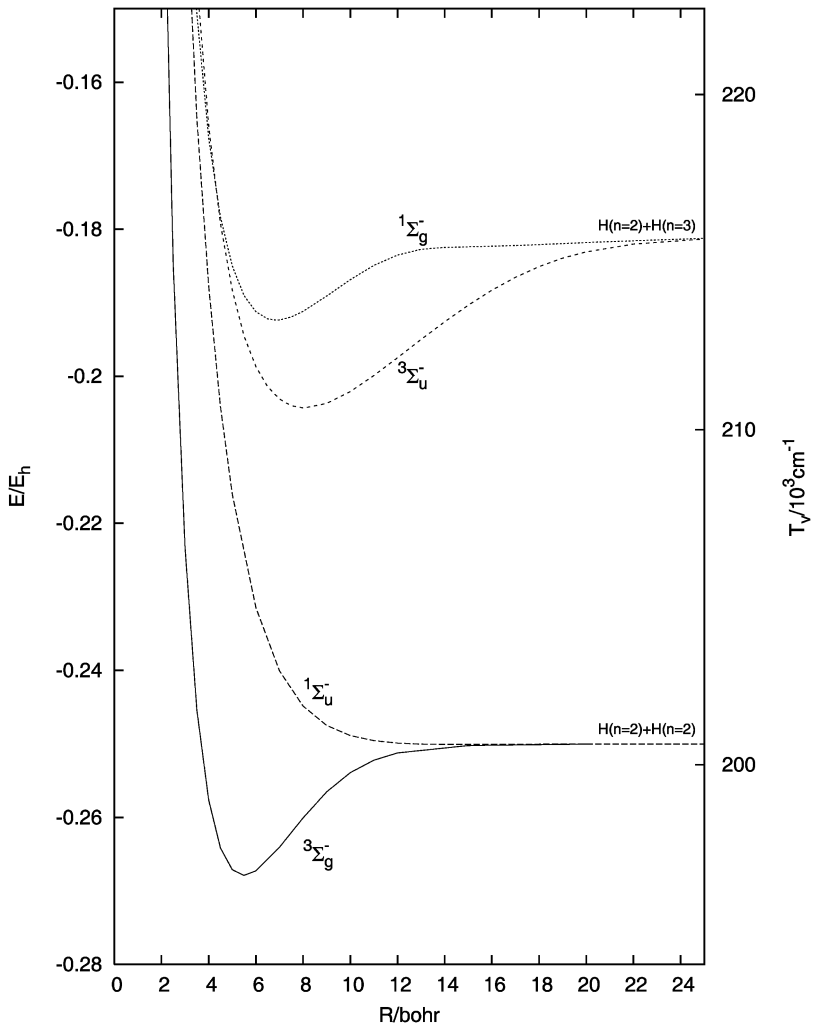

Fig. 2 Detailed view of the Born–Oppenheimer energy curves of the Σ^-states of H_2.

The highest Σ^- state is of singlet *gerade* symmetry. Its minimum at 6.86 bohr lies about 2600 cm^{-1} below the dissociation level. The UA of this state correlates with He($2p3p\,^1$P) of the energy $E = -0.58025\ E_H$[15,16] and the SA limit consists of H($2p$) and H($3p$). The potential is deep enough to accommodate 29 vibrational levels.

The Born–Oppenheimer energy calculated at the limited number of internuclear distances listed in Tables 2 and 3 was employed to create the function $E(R)$ of eqn (2.4)—the potential for the movement of the nuclei. Turning points of this potential were obtained by means of 4-point piecewise polynomial interpolation. The radial nuclear Schrödinger equation has been solved numerically using the Numerov–Cooley–Cashion method[19] as implemented by Le Roy.[20] The integration was performed on a 9000-point grid limited to the range (0;170) bohrs and the nuclear mass set to the proton mass M_p. Results of the vibrational calculations are collected in Table 4. For each vibrational level of a quantum number v, apart from the energy E_v, given relatively to a corresponding dissociation limit, the inertial rotational constant B_v and the leading centrifugal constant D_v are presented. Approximate location of the lowest rotational sublevels can be computed for each rotational quantum number J from the leading terms of the power series expansion

$$E_{v,J} = E_{v0} + B_v J(J+1) - D_v[J(J+1)]^2 + \cdots \quad (3.8)$$

The presence and location of the Σ^- states should be confirmed experimentally, *e.g.* by means of spectroscopic observations. The electronic dipole transition moment $\mu_\parallel(\mu_\perp)$ has the $\Sigma_u^+(\Pi_u)$ symmetry so, as a consequence, the allowed parallel transitions are of $\Sigma^- - \Sigma^-$ type and the perpendicular transitions are of $\Sigma^- - \Pi$ type. Of course, all the other regular selection rules for the parity (*gerade* ↔ *ungerade*) and the spin ($\Delta S = 0$) also limit the possible allowed electronic dipole transitions. On the other hand, the magnetic dipole mechanism makes other transitions weakly allowed, *e.g.* a transition from the lowest $^3\Sigma_g^-$ state to the ground state (X $^1\Sigma_g^+$) could potentially take place. Another factor influencing the intensity of the allowed transitions is the Franck–Condon factor. The overlap between the nuclear wave functions of the initial and target electronic state is likely to be relatively small as the equilibrium distances of the Σ^- states are much larger (see Tables 2 and 3) than those of the lower states (about 2 bohrs).

A good candidate for a relatively intense, allowed transition to be observed is the transition from the $^3\Sigma_g^-$ state to one of the

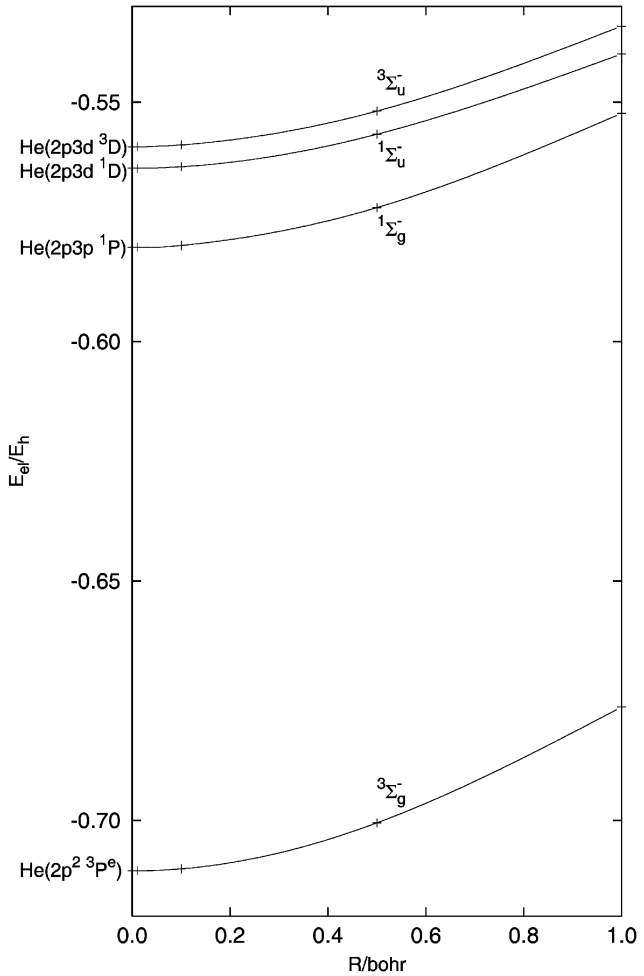

Fig. 3 The short range part of the electronic energy $E_{el}(R)$ of the Σ^- states of H_2. The united atom limit of the electronic energy correlates with the energy of the pertinent excited state of the helium atom.

$^3\Pi_u$ states, for instance, to the metastable levels of c $^3\Pi_u$ state.[21] We also note that the potential energy curve of the k $^3\Pi_u$ state has a shallow (398 cm^{-1}) second minimum at R = 7 bohrs, which is in favour of increasing the Franck–Condon factor.

Rovibronic energy of the Σ^- states is by far in excess of the ionization threshold of H_2 so the spontaneous emission of the electron should be considered as a potential channel of decay. In fact the autoionization process is usually much faster than the radiative decay. This process may occur directly or be preceded by a radiative transition to another autoionizing state of lower energy. From this point of view the Σ^- states of H_2 are not completely stationary although they may be long-lived. Observation of the electron ejected through the autoionization, as well as of the opposite process—the electron scattering, will provide information on the highly excited states.

IV. Conclusion

The Born–Oppenheimer energy curves reported here are of very high accuracy but still several small effects have to be

Table 4 Vibrational energy levels E_v and rotational constants B_v and D_v (eqn (3.8)) of the Σ^-states of H_2 (all in cm^{-1}). The energy E_v is given relative to a corresponding dissociation limit

$^3\Sigma_g^-$

v	E_v	B_v	$-D_v \times 10^4$
0	−3661.3	3.89	8.79
1	−3153.9	3.74	8.76
2	−2672.6	3.58	8.77
3	−2218.9	3.42	8.85
4	−1794.9	3.23	9.03
5	−1403.0	3.03	9.36
6	−1046.8	2.81	9.91
7	−730.6	2.55	10.8
8	−460.4	2.25	12.4
9	−244.0	1.87	15.2
10	−91.1	1.39	21.6
11	−14.0	0.72	36.6
12	−0.1	0.11	98.0

$^1\Sigma_g^-$

v	E_v	B_v	$-D_v \times 10^4$
0	−2415.6	2.50	5.05
1	−2071.8	2.40	5.04
2	−1745.5	2.30	5.06
3	−1438.1	2.19	5.16
4	−1151.5	2.07	5.38
5	−889.0	1.93	5.88
6	−656.2	1.75	7.32
7	−468.2	1.42	14.9
8	−372.2	0.79	11.0
9	−316.6	0.78	6.14
10	−262.2	0.71	2.95
11	−211.9	0.63	3.12
12	−167.1	0.56	3.64
13	−129.5	0.44	8.76
14	−106.5	0.31	3.00
15	−89.1	0.27	2.97
16	−73.9	0.25	2.43
17	−60.2	0.22	1.31
18	−47.9	0.20	1.03
19	−37.0	0.17	1.35
20	−27.7	0.15	1.69
21	−19.8	0.13	1.85
22	−13.4	0.11	1.85
23	−8.41	0.08	1.79
24	−4.75	0.06	1.71
25	−2.29	0.04	1.64
26	−0.84	0.03	1.56
27	−0.17	0.01	1.50
28	−0.01	0.00	1.90

$^3\Sigma_u^-$

v	E_v	B_v	$-D_v \times 10^4$
0	−5065.7	1.82	2.77
1	−4774.7	1.78	2.74
2	−4490.2	1.75	2.70
3	−4212.1	1.71	2.67
4	−3940.4	1.67	2.64
5	−3675.1	1.64	2.61
6	−3416.2	1.60	2.58
7	−3163.8	1.57	2.55
8	−2918.0	1.53	2.52
9	−2678.7	1.50	2.50
10	−2446.0	1.46	2.48
11	−2220.3	1.42	2.46
12	−2001.6	1.38	2.45
13	−1790.2	1.34	2.45
14	−1586.4	1.30	2.46

Table 4 (*continued*)

$^3\Sigma_u^-$			
v	E_v	B_v	$-D_v \times 10^4$
15	−1390.7	1.25	2.48
16	−1203.6	1.21	2.52
17	−1025.9	1.15	2.59
18	−858.4	1.10	2.69
19	−702.4	1.03	2.84
20	−559.5	0.96	3.04
21	−431.5	0.87	3.32
22	−320.5	0.77	3.64
23	−228.5	0.66	4.01
24	−157.6	0.52	5.07
25	−110.7	0.37	5.04
26	−84.0	0.25	3.08
27	−66.9	0.20	1.69
28	−52.8	0.18	1.40
29	−40.7	0.15	1.27
30	−30.5	0.13	1.18
31	−22.0	0.11	1.12
32	−15.1	0.09	1.08
33	−9.70	0.08	1.07
34	−5.67	0.06	1.06
35	−2.89	0.04	1.06
36	−1.18	0.03	1.06
37	−0.31	0.01	1.08
38	−0.02	0.01	1.27

$^1\Sigma_u^-$			
v	E_v	B_v	$-D_v \times 10^4$
0	−5.5	0.48	1.62

taken into account before results of an accuracy comparable with the present day experiment can be obtained. The explicitly correlated wave functions obtained during this project make a good starting point for perturbative computations of adiabatic and nonadiabatic effects, as well as relativistic and radiative corrections. Such a study is underway in our laboratory. Hopefully, this theoretical account will stimulate experimental study on the Σ^- states H_2.

Acknowledgements

I would like to express my gratitude to Krzysztof Pachucki for inspiration and valuable discussions. Computational grant from Poznań Networking and Supercomputing Center is also gratefully acknowledged.

References

1 W. Cencek, J. Komasa and J. Rychlewski, *J. Chem. Phys.*, 1991, **95**, 2572.
2 S. F. Boys, *Proc. R. Soc. London, Ser. A*, 1960, **258**, 402.
3 K. Singer, *Proc. R. Soc. London, Ser. A*, 1960, **258**, 412.
4 W. A. Lester and M. Krauss, *J. Chem. Phys.*, 1964, **41**, 1407.
5 N. C. Handy, *Mol. Phys.*, 1973, **26**, 169.
6 L. Salmon and R. D. Poshusta, *J. Chem. Phys.*, 1973, **59**, 3497.
7 B. Jeziorski and K. Szalewicz, *Phys. Rev. A*, 1979, **19**, 2360.
8 J. Komasa and A. J. Thakkar, *Mol. Phys.*, 1993, **78**, 1039.
9 J. Rychlewski, W. Cencek and J. Komasa, *Chem. Phys. Lett.*, 1994, **229**, 657.
10 M. J. D. Powell, *Comput. J.*, 1964, **7**, 155.
11 J. Komasa, W. Cencek and J. Rychlewski, *Computational Methods in Science and Technology*, Scientific Publishers OWN, Poznań, 1996, vol. 2, p. 87; http://www.man.poznan.pl/cmst.
12 J. Komasa and J. Rychlewski, *Mol. Phys.*, 1997, **91**, 909.
13 W. Cencek, J. Komasa and J. Rychlewski, High-performance computing in molecular sciences, in *Handbook on Parallel and Distributed Processing*, ed. J. Blazewicz, K. Ecker, B. Plateau and D. Trystram, Springer-Verlag, 2000, p. 505.
14 J. Rychlewski and J. Komasa, Explicitly correlated functions in variational calculations, in *Explicitly Correlated Wave Functions in Chemistry and Physics*, ed. J. Rychlewski, Kluwer Academic Publishers, Dordrecht, 2003, p. 91.
15 G. W. F. Drake and A. Dalgarno, *Phys. Rev. A*, 1970, **1**, 1325.
16 H. Doyle, M. Oppenheimer and G. W. F. Drake, *Phys. Rev. A*, 1972, **5**, 26.
17 T. K. Mukherjee and P. K. Mukherjee, *Phys. Rev. A*, 2004, **69**, 064501.
18 S. L. Guberman, *J. Chem. Phys.*, 1983, **78**, 1404.
19 B. Numerov, *Publ. Obs. Central Astrophys. Russia*, 1933, **2**, 188; J. W. Cooley, *Math. Comput.*, 1961, **15**, 363; J. K. Cashion, *J. Chem. Phys.*, 1963, **39**, 1872.
20 R. J. Le Roy, *LEVEL 8.0: A Computer Program for Solving the Radial Schrodinger Equation for Bound and Quasibound Levels*, University of Waterloo Chemical Physics Research Report CP-663, 2007.
21 W. Lichten, *Phys. Rev.*, 1960, **120**, 848.

This paper is published as part of a PCCP Themed Issue on:

Explicit-r_{12} Correlation Methods and Local Correlation Methods

Guest Editors: Hans-Joachim Werner and Peter Gill

Editorial

Explicit-r_{12} correlation methods and local correlation methods
Phys. Chem. Chem. Phys., 2008
DOI: 10.1039/b808067b

Papers

Implementation of the CCSD(T)-F12 method using cusp conditions
Denis Bokhan, Seiichiro Ten-no and Jozef Noga, *Phys. Chem. Chem. Phys.*, 2008
DOI: 10.1039/b803426p

Analysis of non-covalent interactions in (bio)organic molecules using orbital-partitioned localized MP2
Stefan Grimme, Christian Mück-Lichtenfeld and Jens Antony, *Phys. Chem. Chem. Phys.*, 2008
DOI: 10.1039/b803508c

Tighter multipole-based integral estimates and parallel implementation of linear-scaling AO–MP2 theory
Bernd Doser, Daniel S. Lambrecht and Christian Ochsenfeld, *Phys. Chem. Chem. Phys.*, 2008
DOI: 10.1039/b804110e

Local correlation domains for coupled cluster theory: optical rotation and magnetic-field perturbations
Nicholas J. Russ and T. Daniel Crawford, *Phys. Chem. Chem. Phys.*, 2008
DOI: 10.1039/b804119a

Local and density fitting approximations within the short-range/long-range hybrid scheme: application to large non-bonded complexes
Erich Goll, Thierry Leininger, Frederick R. Manby, Alexander Mitrushchenkov, Hans-Joachim Werner and Hermann Stoll, *Phys. Chem. Chem. Phys.*, 2008
DOI: 10.1039/b804672g

Equations of explicitly-correlated coupled-cluster methods
Toru Shiozaki, Muneaki Kamiya, So Hirata and Edward F. Valeev, *Phys. Chem. Chem. Phys.*, 2008
DOI: 10.1039/b803704n

Vanadium oxide compounds with quantum Monte Carlo
Annika Bande and Arne Lüchow, *Phys. Chem. Chem. Phys.*, 2008
DOI: 10.1039/b803571g

Second-order Møller–Plesset calculations on the water molecule using Gaussian-type orbital and Gaussian-type geminal theory
Pål Dahle, Trygve Helgaker, Dan Jonsson and Peter R. Taylor, *Phys. Chem. Chem. Phys.*, 2008
DOI: 10.1039/b803577f

The $^1\Sigma_g^+$ states of the molecular hydrogen
Jacek Komasa, *Phys. Chem. Chem. Phys.*, 2008
DOI: 10.1039/b803548b

Slater-type geminals in explicitly-correlated perturbation theory: application to *n*-alkanols and analysis of errors and basis-set requirements
Sebastian Höfener, Florian A. Bischoff, Andreas Glöß and Wim Klopper, *Phys. Chem. Chem. Phys.*, 2008
DOI: 10.1039/b803575j

Accurate calculations of intermolecular interaction energies using explicitly correlated wave functions
Oliver Marchetti and Hans-Joachim Werner, *Phys. Chem. Chem. Phys.*, 2008
DOI: 10.1039/b804334e

Variational formulation of perturbative explicitly-correlated coupled-cluster methods
Martin Torheyden and Edward F. Valeev, *Phys. Chem. Chem. Phys.*, 2008
DOI: 10.1039/b803620a

Resolution of the identity atomic orbital Laplace transformed second order Møller–Plesset theory for nonconducting periodic systems
Artur F. Izmaylov and Gustavo E. Scuseria, *Phys. Chem. Chem. Phys.*, 2008
DOI: 10.1039/b803274m

On the use of the Laplace transform in local correlation methods
Danylo Kats, Denis Usvyat and Martin Schütz, *Phys. Chem. Chem. Phys.*, 2008
DOI: 10.1039/b802993h

Intracule densities in the strong-interaction limit of density functional theory
Paola Gori-Giorgi, Michael Seidl and Andreas Savin, *Phys. Chem. Chem. Phys.*, 2008
DOI: 10.1039/b803709b

Intracule functional models
Part III. The dot intracule and its Fourier transform
Yves A. Bernard, Deborah L. Crittenden and Peter M. W. Gill, *Phys. Chem. Chem. Phys.*, 2008
DOI: 10.1039/b803919d

Density matrix renormalisation group Lagrangians
Garnet Kin-Lic Chan, *Phys. Chem. Chem. Phys.*, 2008
DOI: 10.1039/b805292c

The interaction of carbohydrates and amino acids with aromatic systems studied by density functional and semi-empirical molecular orbital calculations with dispersion corrections
Raman Sharma, Jonathan P. McNamara, Rajesh K. Raju, Mark A. Vincent, Ian H. Hillier and Claudio A. Morgado, *Phys. Chem. Chem. Phys.*, 2008, **10**, 2767

The principle-quantum-number (and the radial-quantum-number) expansion of the correlation energy of two-electron atoms
Werner Kutzelnigg, *Phys. Chem. Chem. Phys.*, 2008
DOI: 10.1039/b805284k